Dross Formation Mechanisms of Thermally Pre-Treated Used Beverage Can Scrap Bales with Different Density

J. Steglich, R. Dittrich, G. Rombach, M. Rosefort, B. Friedrich, and A. Pichat

Abstract

Used beverage can scrap (UBC) bales can be remelted in state of the art multi-chamber furnaces. Following the recycling of baled UBC scrap in multi-chamber furnaces, a laboratory scale process route was developed for thermal pre-treatment and submerged melting of the scrap. In the present work, UBC scrap types with different densities and level of contamination are compared. The scrap types were thermally pre-treated in different atmospheres up to 823 K (550 °C) and subsequently melted by submerging in a salt-free laboratory process. Melting was performed in pure aluminum at 1023 K (750 °C) under protective argon atmosphere to exclude the influence of thermolysis gases and atmosphere. The impact of remaining organic contamination and oxidation products after thermal pre-treatment on dross formation were described. Results of SEM EDX analysis, as well as thermochemical calculations, were used to explain reactions between solid scrap and the liquid aluminium melt to improve recycling efficiency.

Keywords

Dross formation • UBC • Thermal pre-treatment • Submerged melting

Introduction

This study investigates the impact of thermal pre-treatment on dross formation of used beverage can scrap (UBC). During re-melting of thermally pre-treated UBC scrap, it was found that the pre-treatment can decrease or even increase the amount of dross formation, compared to the un-treated scrap material. This phenomenon is investigated here by combined pre-treatment and submerged melting experiments in laboratory scale.

Two UBC scrap bale qualities with densities of 0.45 and 0.91 t/m^3 were used as raw material. These bales have different levels of contamination, depending of the scrap purity before compacting. The influences of thermal pre-treatment and submerged melting on dross formation are investigated with both scrap types. These process steps are commonly performed and may be combined into one furnace process. The twin-chamber furnace and shaft furnace are two state of the art examples for a combined furnace processes [1]. One goal of this investigation is to describe the impact of organic residue, formed by heating in oxygen containing atmosphere (thermolysis) versus heating in inert-gas atmosphere (pyrolysis).

J. Steglich (✉) · M. Rosefort
TRIMET Aluminium SE, Aluminiumallee 1,
45356 Essen, Germany
e-mail: jan.steglich@trimet.de

R. Dittrich · B. Friedrich
IME Process Metallurgy and Metal Recycling, RWTH Aachen University, Intzestr. 3, 52056 Aachen, Germany

G. Rombach
Hydro Aluminium Rolled Products GmbH,
Georg-Von-Boeselager-Str. 21, 53117 Bonn, Germany

A. Pichat
Parc Economique Centr'alp, Constellium Technology Center,
38341 Voreppe, France

A.P. Ratvik (ed.), *Light Metals 2017*, The Minerals, Metals & Materials Series,
DOI 10.1007/978-3-319-51541-0_133

Literature Survey on Can Coating Reaction Products by Thermal Pre-treatment

In order to describe reaction mechanisms between coating residue of UBC scrap and the liquid melt, a description of this residue is needed. This literature survey focuses on organic coating residue after thermal pre-treatment.

Structure of Thermosetting Can Coating

Waterborne epoxy, polyester and acrylic polymer resins are widely used as beverage can coatings [2–4]. Additionally, phenolic, polyamide and formaldehyde resins are used as crosslinking agents or hardeners for epoxy based coatings [2]. Although a wide variety of coatings and coating mixtures are in use, they are all thermosetting polymers cross-linked into a three-dimensional structure [2, 3, 5]. Bisphenol-a-diglycidylether (BADGE) based epoxy resins are examples for commonly used coating in the can industry. The curing temperature of waterborne resins is in the range of 423–473 K, depending of the resin-cure system and time [2, 3, 6]. In curing, crosslinks are formed and the liquid resin is transformed into a glass-like thermoset. Thermosetting polymers have short sub-chains without rotational freedom and do not become elastic with increasing temperature like thermoplastic resins [5].

Epoxy Polymer Degradation During Thermal Pre-treatment

When the curing temperature of a thermosetting polymer is exceeded, the cross-linked polymer network starts to degrade at the crosslink bonds [5, 7]. The scission of crosslinks leads to reduced crosslink length, resulting a coating with reduced elasticity and hardness [4, 5, 7].

Figure 2 shows the thermogravimetric analysis (TGA) results of two epoxy based can coatings by [4, 7, 8]. The presence of oxygen in the atmosphere determines the decomposition mechanism and how much char is formed. The analysis of [4, 7] are performed with BADGE based epoxy cured with an amine hardener. In investigations of [8], a mixture of BADGE epoxy and phenol-formaldehyde (novolac) resin of ratio 2:1 was used.

Figure 1 shows that polymer degradation in inert gas leads to higher residual char mass, compared to degradation in air or oxygen. Even after heating beyond the liquidus temperature of aluminum, char yields of pure BADGE epoxy were 6.3–7.6% of the initial weight in N_2, compared to 0.1–0.2% heated in air at 1153 K [4]. Whereas [9] reports 1.5 wt% residual char after pyrolysis of pure BADGE epoxy heated in N_2 up to 1073 K.

The solid char residue can be described as an amorphous structure with low crystalline content, featuring porosity and crevices [7, 9, 10]. The char residue of amine cured

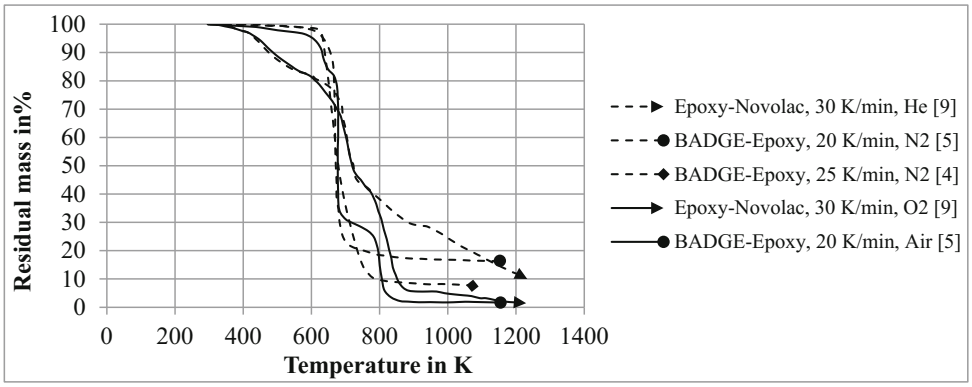

Fig. 1 Comparison of thermogravimetric analysis and temperature depending residual masses of two different epoxy coatings in O_2, air, He and N_2 atmospheres at different heating rates according to [4, 7, 8]

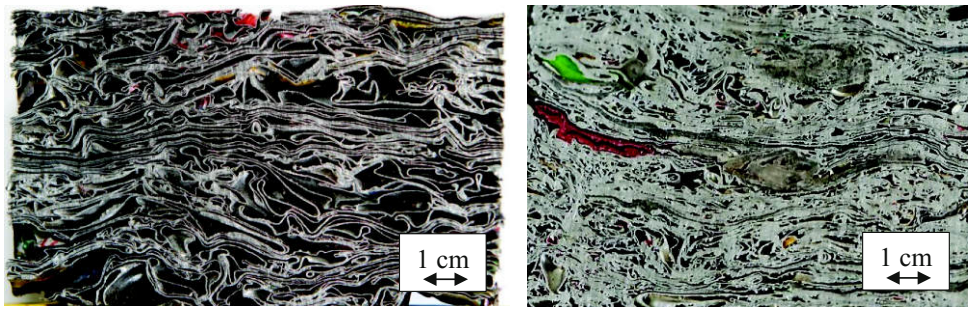

Fig. 2 Detail from UBC material cross sections A (*left side*) and B (*right side*)

BADGE epoxy resin was analyzed by [10], after heating to 1073 K in N_2 flow for a TGA analysis. The results are 84 wt%C, 11 wt%O and 2 wt%N, without traces of sulfur and phosphor. The char residue has a high thermal stability and a low thermal conductivity [10]. Thermal conductivity of epoxy/carbon laminates are measured by [7] to be 8–12 W/mK measured in plane with the laminate and 0.17 W/mK of its solid char, compared to 0.23 W/mK of pure epoxy resin [7].

Experimental Procedure

To investigate the impact of thermal pre-treatment and compacting on dross formation by baled UBC scrap, two scrap types have been characterized, thermally pre-treated, and melted by submerging in pure aluminum melt at laboratory scale.

UBC Material Characterization and Thermal Pre-treatment

Two different commercially available UBC bale qualities are used for the experiments. Table 1 gives an overview of physical bale properties before thermal pre-treatment. UBC material A is a very clean scrap, with a volatile organic content of 2.8 ± 0.3 wt%, showing only minimal other impurities than can coating. The volatile organic content was measured as glowing loss by glowing for 4 h in 773 K hot air on basis of [11]. UBC material B has higher levels of contamination, which are described in Table 1 and shown in Fig. 2.

Figure 2 shows a cross section details from UBC material A and B. The differences in porosity and contamination are visible. The can sheets are commonly made of EN AW-3104 (AlMn1Mg1Cu) and EN AW-5182 (AlMg4.5Mn0.4) alloy.

The two UBC scrap qualities were cut into slices of about 300 mm by 150 mm and 50 mm thickness for thermal pre-treatment. Pre-treatment was performed in an air tight steel cylinder with inner diameter of 260 mm and a height of 445 mm, heated by external resistance heating. To maintain a controlled atmosphere, the scrap was loaded before start of the heating cycle and removed after cooling down. Therefore, a heating ramp with a plateau at the target holding temperature was achieved. The experiments were performed at atmospheric pressure with pure argon, argon with 4 vol.% O_2 and air. Table 2 shows parameters of the thermal pre-treatment. The process temperature and atmosphere represent possible industry conditions.

The temperature distribution in the compacted UBC slices during pre-treatment is assumed to be constant, due to 50 mm thin samples, a low heating rate and use of only one slice per experiment.

Submerged Melting in Laboratory Scale

Following the process route of a twin-chamber process, the pre-treated scrap is melted by submerging into liquid metal, to investigate the dross formation reactions occurring at the liquid metal/solid scrap interface. Therefore, a laboratory scale setup was built to ensure a protective argon atmosphere above the melt during dross formation and to keep the skimming procedure for dross constant. The setup is shown in Fig. 3.

Table 1 Physical UBC scrap bale properties before thermal pre-treatment

Property	Unit	UBC A	UBC B	Method of analysis
Major impurities	–	Coating	Coating, plastic, iron, copper	Visual
Density	kg/m^3	450	910	Weighing
Volatile organic content	wt%	2.8 ± 0.3	8.4 ± 4.0	Glowing loss
Moisture content	wt%	0.9 ± 0.7	1.7 ± 1.1	Drying
Porosity	%	83	66	Calculated

Table 2 Experiment parameters of thermal pre-treatment in laboratory scale steel cylinder

Experiment	Atmosphere at 1 atm	Gas flow in l/min	Heating ramp in K/min	Cooling ramp in K/min	Holding temperature in K	Holding time in min
Argon	Argon	10	5	2–3	823 ± 5	30 ± 5
Argon + $4O_2$	Argon + 4 vol. % O_2	10	5	2–3	823 ± 5	30 ± 5
Air 823 K	Air	10	5	2–3	823 ± 5	30 ± 5
Air 723 K	Air	10	5	2–3	723 ± 5	30 ± 5
Raw	Only pre-dried raw UBC material					

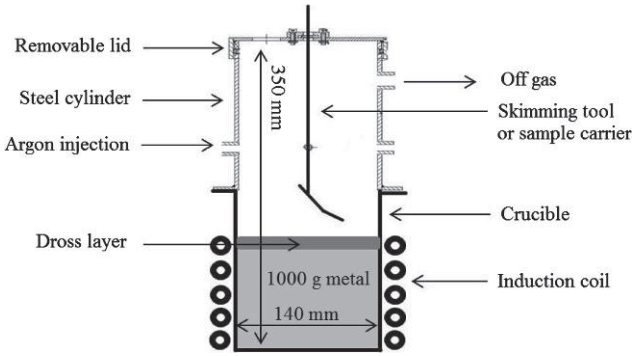

Fig. 3 Schematic laboratory scale setup for dross formation experiments by submerged melting of UBC in argon inert gas

For each experiment, 1000 ± 5 g of Al 99.9 metal were molten in a $SiO–Al_2O_3$ crucible. When the metal reached 1023 ± 5 K, a thin pristine dross layer was skimmed off, and 100 ± 1 g UBC scrap were attached by aluminum-wire to a sample carrier tool. The sample was placed in the steel cylinder with argon atmosphere and the lid was closed. A purge time of two minutes achieved an O_2 concentration below 100 ppm in the atmosphere. All pre-treated UBC samples were submerged in 5–10 s into the melt. After 5 min reaction time, the carrier tool was exchanged against a skimming tool (shown in Fig. 3) and the dross layer was visually inspected to ensure complete melting of the scrap, otherwise stirred manually once. An additional 30 min reaction time in argon atmosphere were maintained. Finally, the dross was skimmed, cooled in argon, weight and analyzed. The experiments were performed three times for each condition with new metal heals.

Dross formation is calculated, as usual in the industry [1], in relation to the scrap input mass, according to Eq. 1. The non-metallic particle (NMP) content is measured by remelting under salt flux and calculated by Eq. 2:

$$\text{Dross in } \% = \frac{\text{dross mass}}{\text{dry scrap mass}} * 100 \quad (1)$$

$$\text{NMP in } \% = \frac{\text{dross mass} - \text{recovered metal mass}}{\text{dross mass}} * 100 \quad (2)$$

For analysis, the non-metallic-particle content of the skimmed dross was measured by remelting under salt flux (equimolar NaCl:KCl flux with 5 wt% added cryolite) in a scrap to salt ratio of 1:2 at 1023 K. After the salt was liquid, the dross was added and molten for 40–50 min under repeated stirring. Carbon and oxygen concentrations in the UBC material were measured by the total combustion method with a Leco TC600 and Leco TOS800. The samples were taken as drilling swarf spot samples from each material by nine spot samples for each UBC scrap material. As a result, a total of 90 carbon and oxygen samples of UBC scrap were analyzed. With this scrap material, 30 dross formation experiments have been performed.

Results and Discussion

The total carbon and oxygen content remaining on the can sheets is used to rate the success of organic removal while preventing oxidation of the material. Afterwards, the dross structures are analyzed for reaction products and set into context with the dross formation masses.

Influence of Thermal Pre-treatment on Carbon and Oxygen Content of Baled UBC Scrap

Figure 4 shows a significant difference in carbon and oxygen content of UBC material A and B after thermal pre-treatment. There is a strong reduction of carbon and oxygen of UBC material A under all thermolysis (substoichiometric oxygen in atmosphere) and pyrolysis (absence of oxygen) conditions used. For UBC A, pyrolysis with argon at 823 K leads to the highest concentration of C and O remaining on the scrap. In contrast, thermolysis in air at 823 K, leads to the highest removal of C (0.04 wt% left) and less O than in the raw material. Oxygen concentration is decreased as well, due to the presence of oxygen in volatiles.

On the other hand, C and O removal of material B was not as significant. A comparison of sample B Raw with the remaining B series samples shows a reduction of carbon content. The lowest remaining carbon concentration of UBC material B was also achieved by thermolysis in air at 823 K, but the highest oxidation as well. The thermolysed samples show higher concentrations of oxygen than the raw material. Even though an increase in reactor temperature or off gas temperature during thermal pre-treatment was not measured, an exothermic reaction of the plastic content could have raised the temperature in the bale locally, resulting in oxidation. This is supported by the lower O concentration of material thermolysed at 723 K in air. Humidity in material B was also higher, which can initiate earlier oxidation [12]. Temperature dependent oxidation reactions and kinetics are described in studies of [12, 13].

The main difference of the can sheet is shown in Fig. 5, as taper-section of AlMn1Mg1Cu can sheet after pyrolysis (sample A Argon) by an optical microscope image. A continuous coating residue layer was observed. The image is overexposed to highlight the can coating. No residual coating layer was visible on the thermolysed sample A Air 823 K.

Pyrolysis lead to the transformation of can coating to a 1–3 µm thick char layer on can body sheets and 3–4 µm

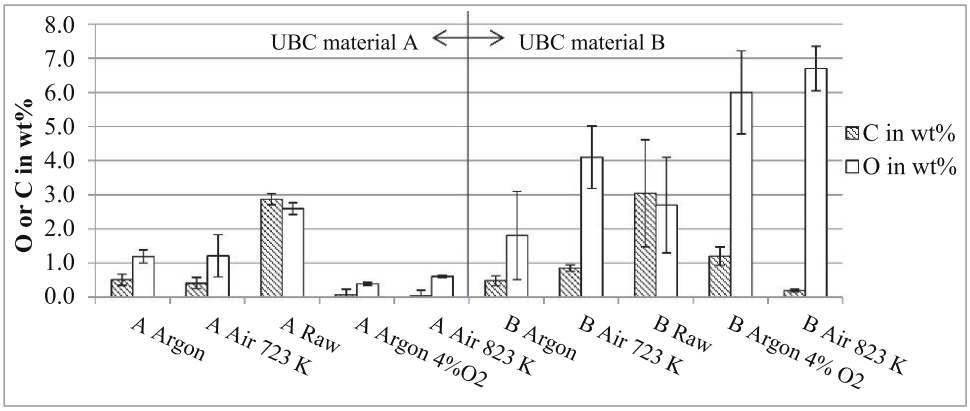

Fig. 4 Carbon and oxygen concentration in compacted UBC material A and B, taken as spot samples by drilling from one slice for each type after thermal pre-treatment

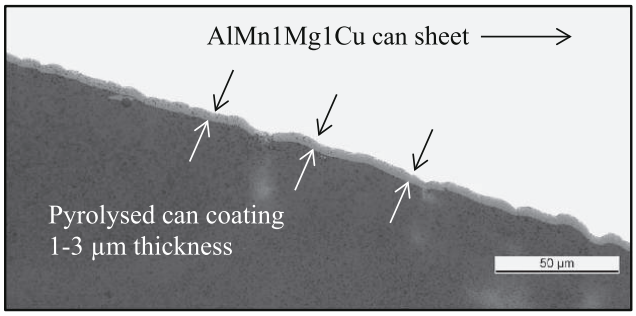

Fig. 5 Polished taper sections as optical microscopic image of can body sheets after pyrolysis and heating by 5 K/min to 823 K in argon

thick layer on can ends and. The thermolysis samples of scrap A and B show almost complete removal of the coating on can ends and sheet, with scattered pits and pores, indicating starting oxidation, but no severe oxidation products by break-away oxidation. These features are also identified by SEM EDX analysis in the solidified dross samples after submerged melting.

Influence of Scrap Bale Density and Pre-treatment on Dross Formation

The skimmed dross was cooled, weight, and remelted under salt. The results of generated dross mass and non-metallic-particle (NMP) content are shown in Fig. 6. The dross formation masses are higher than in industry processes, due to effect of laboratory scale and skimming procedure. Material A shows a significantly reduction of dross formation by thermolysis at 823 K, as expected by the low C and O concentrations.

Submerged melting of pyrolysed UBC A produced more dross compared to untreated material, due to the adhering char residue on the can sheets. The effect is explained in detail in Sect. "Influence of Thermal Pre-treatment on Dross Structure and Reactions".

For material B the results show no significant difference in dross formation after thermal pre-treatment. The major differences in material A and B are the higher density and level of contamination of scrap B. This can be explained by

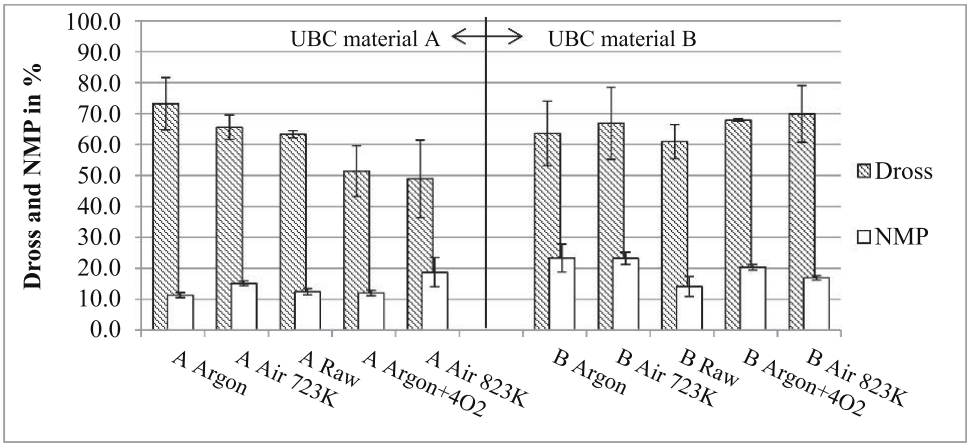

Fig. 6 Dross formation mass and NMP content of dross generated by three experiments with 100 g of each UBC scrap type, sorted by formed dross mass

the higher level of organic residue on the scrap of UBC material B, indicated by C and O levels (Fig. 4).

By incomplete removal of organic residue, it is concluded that the higher density impeded the organic removal as gaseous pyrolysis/thermolysis products through smaller tortuous pores. Therefore, a higher compaction rate seems not beneficial, if organics have to be removed as gaseous products. These results are not contrary to findings of [14, 15], using washed and pre-dried aluminum swarf with usual volatile content below 0.2 wt%.

Influence of Thermal Pre-treatment on Dross Structure and Reactions

Cross sections of dross samples were ground, polished and investigated by optical microscopy followed by SEM EDX analysis. For the SEM EDX analysis, the samples were additionally ion-polished in vacuum, to exclude carbon contamination. Figure 7 shows the SEM image of dross sample A Raw in BSE mode. Dark regions have lower atomic number, bright regions higher.

Figure 7 shows bright regions of pure aluminum (spectrum 1) used as metal heal in the experiment, which surrounds an aluminum-oxide "*bi-film*" [16] (spectrum 4). The bi-film originates from the can sheet alloy, as the presence of Mg indicates. The bi-film is present on the can sheets as natural oxide or by oxidation during pre-treatment according to reaction 3–5. All ΔG values of the following reactions were calculated with the reaction module of FactSage Version 7.0 [17] at the indicated temperature. The activities of alloying elements are calculated with the Equilib module, based on a 3:1 mixture of can body to can end alloy. Activities of O_2 are based on the partial pressure of 4 vol.% O_2 at atmospheric pressure, all other adducts are set to 1.

$$1/2\mathrm{Mg} + \mathrm{Al} + \mathrm{O_2} = 1/2\mathrm{Al_2MgO_4} \quad \Delta G_{723/823\mathrm{K}} = -970/-945\,\mathrm{kJ/mol} \tag{3}$$

$$2\,\mathrm{Mg} + \mathrm{O_2} = 2\,\mathrm{MgO} \quad \Delta G_{723/823\mathrm{K}} = -986/-955\mathrm{kJ/mol} \tag{4}$$

$$4/3\mathrm{Al} + \mathrm{O_2} = 2/3\,\mathrm{Al_2O_3} \quad \Delta G_{723/823\mathrm{K}} = -946/-922\,\mathrm{kJ/mol} \tag{5}$$

Spectrum 4 shows C and S present in the oxide film, indicating organic residue. C could be present atomic or as Al_4C_3 from reaction 8 during dross formation. Spectrum 2 shows similar elements, but O and C in much higher concentration in a larger region with a defined shape. Using 5 kV voltage for EDX analysis, the interaction volume has a diameter smaller than 1 µm. Therefore, all elements can be present in the area of particle (2). Reactions 6–8 yield products that can be present simultaneously.

$$4/3\mathrm{Al} + 2/3\mathrm{MgO} + \mathrm{O_2} = 2/3\mathrm{Al_2MgO_4} \quad \Delta G_{1023\mathrm{K}} = -896\,\mathrm{kJ/mol} \tag{6}$$

$$2\,\mathrm{Mg} + \mathrm{O_2} = 2\,\mathrm{MgO} \quad \Delta G_{1023\mathrm{K}} = -885\,\mathrm{kJ/mol} \tag{7}$$

$$4/3\mathrm{Al} + \mathrm{C} = 1/3\,\mathrm{Al_4C_3} \quad \Delta G_{1023\mathrm{K}} = -150\,\mathrm{kJ/mol} \tag{8}$$

Region (3) with spectrum 3 shows a porous, foam-like structure with internal porosity and high amounts of O, Mg and C. The porous structure implies the involvement of reactive gases as described in reactions 3–7 or the solid oxidation of magnesium according to

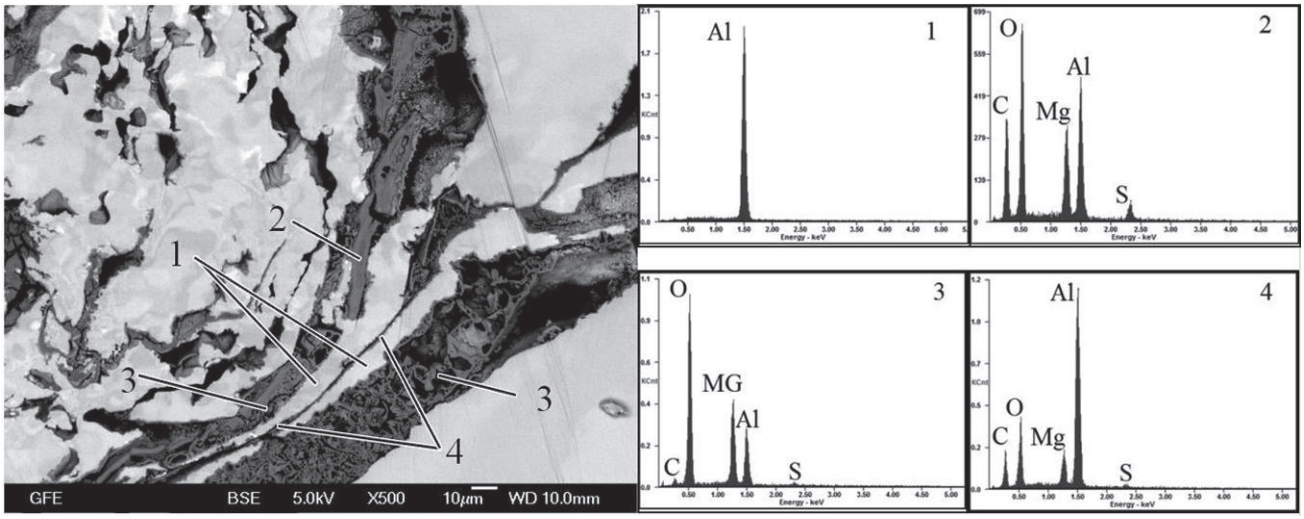

Fig. 7 SEM image of dross sample a raw with according EDX spectra on the *right*

$$4/3\gamma Al_2O_3 + Mg = 2/3Al + Al_2O_4Mg \quad G_{1023K} = -52\,kJ/mol \tag{9}$$

$$MgO + \gamma Al_2O_3 = Al_2MgO_4 \quad \Delta G_{1023K} = -44\,kJ/mol \tag{10}$$

Sample A Argon is analyzed in Fig. 8. Unfortunately, the ion-polishing deposited aluminum material in the porosity of the dross. Nevertheless, the pyrolysed can coating residue is visible in the dross matrix after 30 min at 1023 K, stirred in a 10 kHz induction furnace and forced submerged melting.

Figure 8 shows pyrolysed char residue of can coating with defined shape, featuring sharp edges at the cracks, indicating a brittle material, as described in Sect. "Epoxy Polymer Degradation During Thermal Pre-treatment". White TiO_2 pigments are passivated in the coating layer, which can be reduced by aluminum if the char has cracked. Region 1 shows Mg, Si and O present together, which can be formed a local enrichment in Mg and Si, as by dissolving Mg_2Si phases, which are present in 5000 series alloy systems [16], according to Eq. 11. This phase oxidation has to be verified in future work.

$$Mg_2Si + O_2 = 2\,MgO + Si \quad \Delta G_{823/1023K} = -917/-866\,kJ/mol \tag{11}$$

In sample A Argon, pores have formed directly at the pyrolysed coating. The low wetting of aluminum and carbon [16] promotes the separation of aluminum matrix and the oxide films, resulting in porosity in between the bi-films. [16]. Without wetting, coalescence of entrapped aluminum is impeded.

This observation is confirmed by Fig. 9, showing metal penetrating through oxide films in the polished cross section of sample A Air 823 K. The folded oxide films have started to fragmentize by penetrating metal during dross formation. The fragmentation is necessary to promote coalescence of the liquid metal. The oxide films coagulate with other oxides, as refractory or the dross layer on the liquid metal.

Deduction of Dross Formation Mechanisms and Summary

Following the twin-chamber process organically contaminated used beverage can (UBC) scrap bales have been thermally pre-treated and melted by submerging in Al99.9 in laboratory scale. Thermal pre-treatment was performed under argon atmosphere (pyrolysis) and oxygen containing atmospheres (thermolysis) in air at 723 and 823 K at atmospheric pressure.

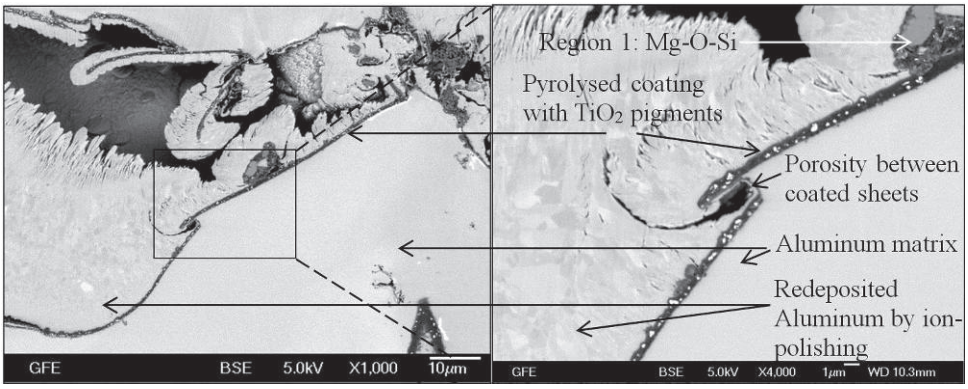

Fig. 8 SEM image of dross sample A Argon after ion-polishing with enlarged section on the *right side*. The dark char residue is visible with *white pigments* incorporated

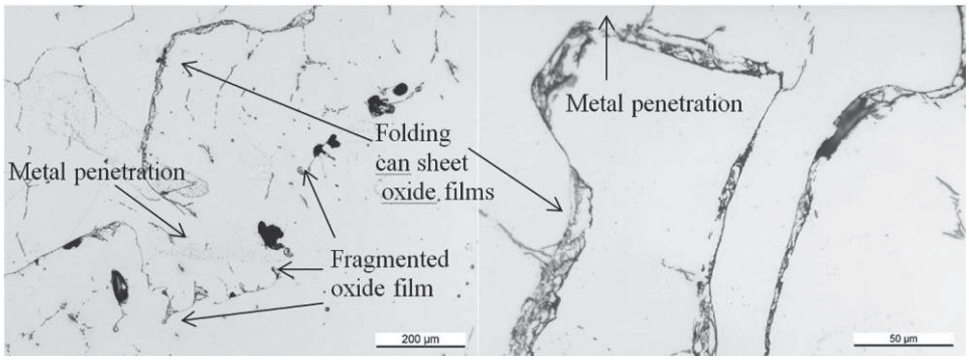

Fig. 9 Light optical image of polished cross section from sample A Air 823 K. Oxide film residues of can sheets are visible in the aluminum matrix

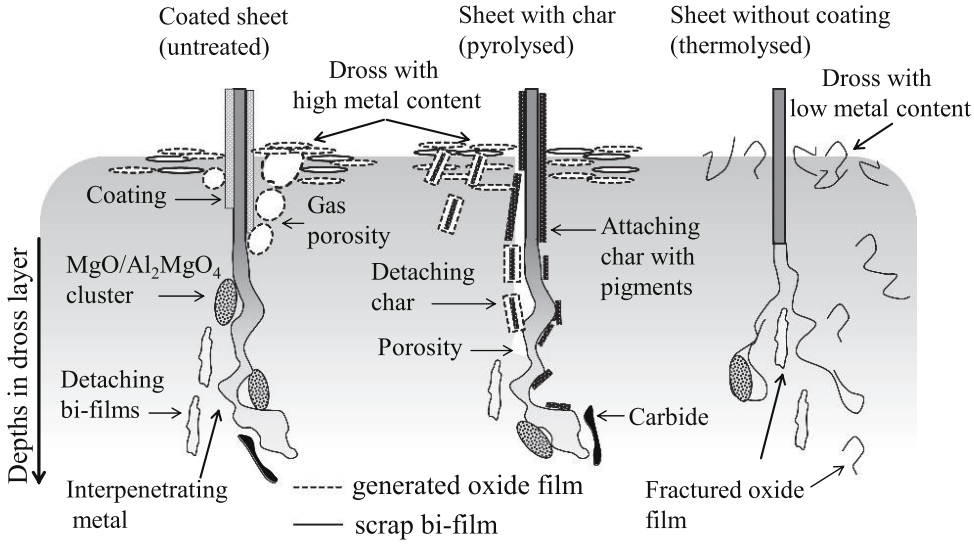

Fig. 10 Proposed dross formation mechanisms of coated can sheet with and without thermal pre-treatment based on microscopic- and SEM EDX-results

The UBC material with a density of 450 kg/m^3 and a volatile organic content of 2.8 ± 0.3 wt% responded with significant difference in organic removal to the thermal pre-treatment. The lowest dross formation and oxidation of the material were achieved by thermolysis with argon + 4 vol.% O_2 at 823 K (Fig. 6), a heating ramp of 5 K/min and 30 ± 5 min at target temperature. Under the assumption that closed porosity in an idealized bale of clean sheets is filled with oxygen containing air, this bale would generate comparable amounts of dross. Pyrolysis under pure argon and equivalent heating conditions increased the dross formation in comparison to the untreated material. This is caused by pyrolysed coating char residue, adhering to the metal sheets, even after forced submerging and a reaction time of 30 ± 5 min at 1023 K in a stirred laboratory induction furnace. Consequently, the pyrolysis process leads to reinforced composite "*bi-films*" [16] supporting their structure. The described dross formation mechanisms are summarized in Fig. 10.

In contrast, the UBC B with a higher density of 910 kg/m^3 and high volatile organic content of 8.4 ± 4.0% does show an increased oxygen content after thermolysis. The oxidation is possibly caused by locally exothermic reactions of the plastic content and moisture in the scrap. In combination with the smaller pores, which impede gas transport out of the bale structure, the removal of organic contamination was not successful. Therefore, thermal pre-treatment of this UBC material shows no significant reduction of dross formation.

In future work, the reaction kinetics of different carbon qualities, as for example the amorphous residue of can coating should be investigated at different temperatures. This investigation should explain the conditions necessary to induce carbide formation.

Acknowledgements The research leading to these results has been carried out within the framework of the AMAP (Advanced Metals And Processes) research cluster at RWTH Aachen University, Germany. We like to thank Aleris Rolled Products Germany GmbH, Constellium, Hydro Aluminium Rolled Products GmbH and Trimet Aluminium SE for financial support of this research. Furthermore, the Bachelor Thesis of student Fabio Rühl is gratefully acknowledged.

References

1. K. Krone (ed.), *Aluminiumrecycling: Vom Vorstoff bis zur fertigen Legierung* (Düsseldorf, VDS e. V., 2000), pp. 101–370
2. J.V. Koleske (ed.), *Paint and Coating Testing Manual* (ASTM Manual Series: MNL 17, Philadelphia, PA, 1995), pp. 53–106
3. D. Stoye (ed.), *Paints, Coatings and Solvents* (VCH Publishers, Weinheim, 1993), pp. 1–10
4. A. Gu, G. Liang, Thermal degradation behavior and kinetic analysis of epoxy/montmorillonite nanocomposites. Polym. Degrad. Stab. **80**(2), 383–391 (2003)
5. R.F.T. Stepto, *Polymer Networks Principles of their Formation, Structure and Properties* (Thomson Science, London, 1998), pp. 1–289
6. H. Stutz, K.H. Illers, J. Mertes, A generalized theory for the glass transition temperature of crosslinked and uncrosslinked polymers, J. Poly. Sci. Part B Poly. Phys. **28**, 1283–1498 (1990)
7. A.P. Mouritz, A.G. Gibson, *Fire Properties of Polymer Composite Materials* (Dordrecht, The Netherlands, 2006), pp. 32–38
8. W. Kaiser (ed.), *Kunststoffchemie für Ingenieure* (Carl Hanser Verlag GmbH, München, 2011), pp. 409–444
9. A. Mlyniec, J. Korta, T. Uhl, Structurally based constitutive model of epoxy adhesives incorporating the influence of post-curing thermolysis, *Composites Part B*, vol. 86 (2016), pp. 160–167
10. M.-J. Xu et al., Synthesis of a cross-linked triazine phosphine polymer and its effect on fire retardancy, thermal degradation and moisture resistance of epoxy resins. Polym. Degrad. Stab. **119**, 14–22 (2015)
11. DIN 18128:2002–12, *Soil—Investigation and Testing—Determination of Ignition Loss* (2002)
12. D. Stevens et al., Oxidation of AlMg in dry and humid atmospheres, *Light Metals* (2011)

13. S.A. Impey, The mechanism of dross formation on aluminium and aluminium-magnesium alloys. Ph.D. Thesis, Cranfield institute of technology (1989)
14. H. Paulitsch, H. Antrekowitsch, A. Schmid, Vergleich des Abbrandverhaltens beim Rezyklieren von Aluminiumspänen und –briketts, BHM. **156**(1), 6–13 (2011)
15. H. Puga et al., Recycling of aluminium swarf by direct incorporation in aluminium melts. J. Mater. Process. Technol. **209**, 5195–5203 (2009)
16. J. Campbell, *Complete Casting Handbook* (Oxford, Elsevier Ltd., 1998), pp. 3–103
17. W. Bale et al., *FactSage 7.0* (Thermfact Ltd, GTT–Technologies, 2016)
18. T. Ahamad, S. Alshehri, Thermal degradation and evolved gas analysis of epoxy (DGEBA)/novolac resin blends (ENB) during pyrolysis and combustion. J. Therm. Anal. Calorim. **111**, 445–451 (2013)